Compensation of Tool Axis Misalignment in Active Magnetic Bearing Spindle System

Chong-Won Lee*, Yeo-Kwon Yoon and Ho-Seop Jeong*****

(Received June 8, 1996)

The tool axis misalignment, which causes machining inaccuracies in an active magnetic bearing(AMB)-spindle system, can be compensated by tracking control of the rotor-spindle. The pseudo-derivative feedback(PDF) control scheme alone does not correct the tool axis misalignment since the integral action results in the narrow bandwidth and large phase lag in the controlled system. To improve the tracking performance, the feedback and feedforward controllers are combined with the existing proportional-derivative controller, which stabilizes the inherently unstable AMB-spindle system dynamics. The theoretical and experimental results show that proposed control scheme efficiently compensates the tool axis misalignment compared with the conventional PDF control scheme.

Key Words: Active Magnetic Bearings, Misalignment, Pseudo-Derivative Feedback Controller, Feedforward Control

1. Introduction

The tool axis misalignment, which may be inevitable due to frequent tool changes in machining process such as milling and grinding, often leads not only to machining inaccuracies but severe machine vibrations due to the imbalance of the high speed spindle. Unlike a spindle supported by rolling element bearings, active magnetic bearings (AMBs) inherently have the ability to compensate for such tool axis misalignment within the air gap between the spindle shaft and the emergency bearing by tracking control of the spindle shaft. The whirling motion of the parallel misaligned tool center is synchronous to the spindle rotational speed (Siegwart et al., 1990 and Ota et al., 1990). Thus, the AMBs, in addition to supporting the shaft, should operate as an actuator of a wide frequency bandwidth and a small phase lag to reduce the whirling motion. So far, the compensation of tool axis misalignment using AMBs has not yet been addressed in the literature. However, a few works have been reported on the use of electromagnetic actuators to improve the machining accuracy. For example, Möller has developed a boring system equipped with an electromagnetic actuator, which can machine elliptic pin holes of engine pistons by modulating the spindle speed and the deflection of tool edge. The elliptic bore was 50μm off from the cylindrical bore of 20~30mm diameter (Möller, 1990)

In this work, AMB-spindle system is modeled as a single-DOF system and the pseudo-derivative feedback (PDF) controller is designed to stabilize the AMB-spindle system and to achieve the desired tracking performance. But the PDF-controlled system has undesirable characteristics such as a narrow frequency bandwidth and a large phase lag. It necessitates the addition of a feedforward controller to improve the tracking performance. The feedforward controller is constructed by

* Center for Noise and Vibration Control, Department of Meachanical Engineering, KAIST, Science Town, Taejon, 305-701, KOREA
** Central Research Institute, Samsung Heavy Industry P. O. Box 43, Science Town, Taejon, 305-600 KOREA
*** Research & Development Center, Samsung Electro-Mechanics, 314, Maetan 3 Dong Paldal Ku, Suwon Si, Kyungki Do, 441-743, KOREA

inverting the AMB-spindle system dynamics which was stabilized by a PD-controller only. The experimental results show that the proposed control scheme effectively compensates for the tool axis misalignment compared with the conventional PDF control scheme.

2. Modeling of AMB-Spindle System

For a typical four axes rigid rotor-AMB system model as shown in Fig. 1, it is well known that the mass matrix is coupled at bearings #1 and #2, and the gyroscopic effect is coupled in the y and z-directional motions. In practice, however, the gyroscopic effect is likely to be smaller than the controlled damping, and the off-diagonal elements of the mass matrix are negligibly small (Delprete et al., 1994 and Kim, 1995). As the results, the coupled 4-DOF AMB system model can be decoupled as four single-DOF system models. The equation of motion of a single-axis magnetic bearing system can be written, using the linearized magnetic force, as

$$m\ddot{q}-K_q q=K_{iq}i_q, \quad q=y_1,\ y_2,\ z_1,\ z_2 \quad (1)$$

where

$$K_q=\left(\frac{\partial F_q}{\partial q}\right)_{iq=q=0}=\frac{c\alpha\mu_o N^2 A_p(I_{o1}^2+I_{o2}^2)}{2g_o^3}$$

$$K_{iq}=\left(\frac{\partial F_q}{\partial i_q}\right)_{iq=q=0}=\frac{\alpha\mu_o N^2 A_p(I_{o1}+I_{o2})}{2g_o^2}$$

$$\alpha=\frac{sin\beta_2-sin\beta_1}{\beta_2-\beta_1}, \qquad c=\frac{cos\beta_1+cos\beta_2}{2}$$

Here m is the equivalent mass in the bearing coordinate; K_q is the position stiffness; K_{iq} is the current stiffness; α and c are the geometric factor for displacement and force, respectively; β_1 and β_2 are the angles from the center line of magnetic poles to the near an far edges of the pole face, respectively; μ_o is the permeability in free space ($4\pi\times10^{-7}$H/m); N is the number of coil turns; A_p is the pole face area; I_{o1} and I_{o2} are the bias currents at magnet 1 and 2, respectively; ig is the control current; g_0 is the steady state air-gap. As shown in Eq. (1), the AMB system has the negative stiffness, so the stabilization control of the current in the electromagnets is always reguired by implementing double acting magnets. The rotor position is continually monitored by a proximity sensor and the position signal is transformed into a control signal, which controls the current of the electromagnet. However, since the controller ouput is voltage, the relation between the control voltage and the control current of electromagnet should be considered. The self inductance of coil induces a time delay between the control voltage and the control current, which may destabilize the system. To improve this problem the current feedback scheme is introduced, and then voltage-current relation can be written as

$$\tau_c\frac{di_q}{dt}+i_q=K_c u_q-\frac{\gamma K_{iq}}{K_a R_f+R}\frac{dq}{dt}$$

$$K_c=\frac{K_a}{K_a R_f+R}, \quad \tau_c=\frac{L_0}{K_a R_f+R}$$

$$\gamma=\frac{c}{2\alpha} \quad (2)$$

where u_q is the control voltage; K_a is the voltage gain of the power amplifier; R_f is the current feedback gain; R is the sum of resistances of the coil and the current detector; L_0 is the nominal inductance; K_c is the voltage-to-current gain; τ_c is the time constant of coil with current feedback.

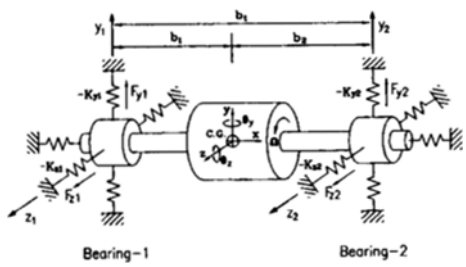

Fig. 1 Rigid-rotor active magnetic bearing system model

3. Controller Design

To compensate for the misalignment between the spindle shaft and the tool, the control inputs, which are synchronized to the spindle speed, are applied to the system. It requires that the controlled system should have the wide frequency bandwidth well over the maximum spindle speed and the small phase lag between the input and output.

3.1 PDF controller

Neglecting the small time constant of coil with current feedback, τ_c, we can simplify the relation between the control voltage, $U_q(s)$, and the displacement voltage, $V_q(s)$, as

$$G(s)=\frac{V_q(s)}{U_q(s)}=\frac{K_cK_sK_{iq}}{ms^2-K_q} \tag{3}$$

where K_s is the displacement sensor gain. The corresponding state-space equation becomes,

$$\begin{aligned} \boldsymbol{X}_p &= \boldsymbol{A}_p\boldsymbol{X}_p+\boldsymbol{B}_pu_q \\ Y_p &= \boldsymbol{C}_p\boldsymbol{X}_p \end{aligned} \tag{4}$$

where

$$\boldsymbol{X}_p=[v_q \quad \dot{v}_q]^T$$
$$\boldsymbol{A}_p=\begin{bmatrix} 0 & 1 \\ K_q/m & 0 \end{bmatrix},\ \boldsymbol{B}_p=\begin{bmatrix} 0 \\ K_cK_sK_{iq}/m \end{bmatrix}$$
$$\boldsymbol{C}_p=[1 \quad 0]$$

When a PD-controller is used to stabilize the inherently unstable AMB system, the steady-syate position error may occur in case of tracking control. To eliminate the steady-state error, an integral action is added to the existing PD- controller as shown in Fig. 2(a). The integrator

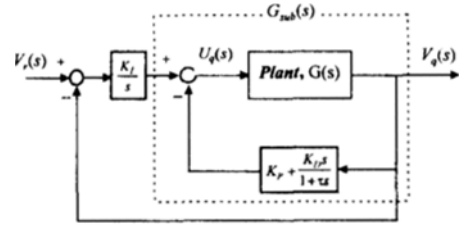

(a) PDF controlled system

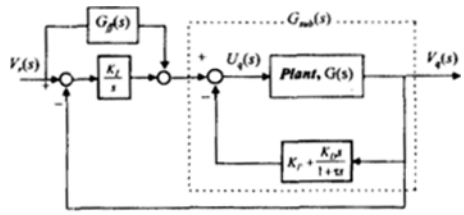

(b) PDF controlled system with feedforward controller

Fig. 2 Controlled structure for tracking control: $\tau(=3.3\times10^{-4}$sec) is the time constnt of low-pass filter for reducing the efect of noise in the differentiator.

dynamics is written as

$$\dot{X}_I=Y_P \tag{5}$$

Introducing the new state variable (Takita and Seto, 1991), $\boldsymbol{X}=[X_I \quad \boldsymbol{X}_P]^T$, we can write Eq. (4) as

$$\begin{aligned} \dot{\boldsymbol{X}} &= \boldsymbol{A}\boldsymbol{X}+\boldsymbol{B}u_q \\ Y &= \boldsymbol{C}\boldsymbol{X} \end{aligned} \tag{6}$$

where

$$\boldsymbol{A}=\begin{bmatrix} 0 & \boldsymbol{C}_P \\ 0 & \boldsymbol{A}_P \end{bmatrix},\ \boldsymbol{B}=\begin{bmatrix} 0 \\ \boldsymbol{B}_P \end{bmatrix},\ \boldsymbol{C}=[0 \quad \boldsymbol{C}_P]$$

Now consider the quadratic performance index given by

$$J=\int_0^\infty(\boldsymbol{X}^T\boldsymbol{Q}\boldsymbol{X}+u_q^T\boldsymbol{R}u_q)dt \tag{7}$$

where $\boldsymbol{Q}$ and $\boldsymbol{R}$ are the positive semi-definite and positive definite weighting matrices, respectively. Then the optimal control law can be obtained as follows by minimizing J;

$$\begin{aligned} u_q &= -\boldsymbol{R}^{-1}\boldsymbol{B}^T\boldsymbol{P}\boldsymbol{X} \\ &= -\boldsymbol{K}_{opt}\boldsymbol{X}=-[K_I \quad K_P \quad K_D]\boldsymbol{X} \end{aligned} \tag{8}$$

where $\boldsymbol{P}$ is the solution of an algebraic matrix Riccati equation.

The weighting matrices are determined such that unstable responses due to saturation of the supply voltage and flux density are not observed. In order to design a fast tracking system, the

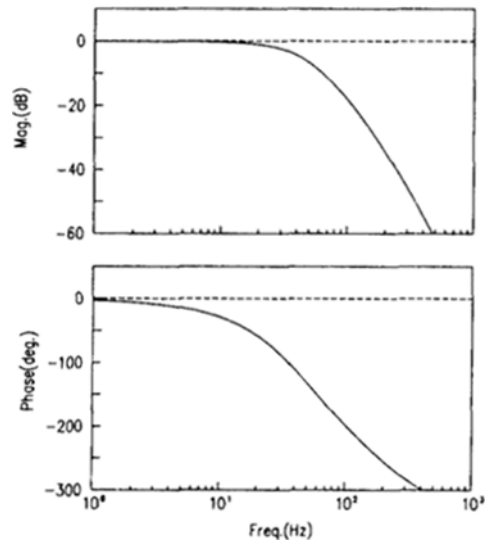

Fig. 3 Frequency response function of the overall system: without feedforward; with feedforward

relative weight of integral terms should be increased. However, an excessive weighting induces the instability due to saturation of the supply voltage and flux density. For the weighting matrices given by

$$\boldsymbol{Q}=diag[9\times10^{4},\ 0.5\times10^{-1},\ 0.5\times10^{-8}]$$
$$\boldsymbol{R}=1 \tag{9}$$

the optimal control gain matrix is mdetermined as

$$\boldsymbol{K}_{opt}=[K_I\ \ K_P\ \ K_D]$$
$$=[300\ \ 3.4\ \ 0.0081] \tag{10}$$

resulting in the dominant closed loop poles at $-575.9\ \pm j328.9$[rad/sec], and the damping ratio of $\zeta=0.87$. Figure 3 shows the FRF of the PDF-controlled system. Note that the steady-state error is almost 0 in the frequency range below 10Hz, whereas the tracking performance becomes poor in the frequency range beyond 10Hz.

3.2 Feedforward controller

In order to improve the narrow frequency bandwidth and large phase lag, resulting from the PDF controller, a feedforward controller is added as shown in Fig. 2(b). The feedforward control is used to anticipate the effects of a command input on the process output and to modify manipulations generated by a closed-loop control system in such a way that the error in the process output is reduced (Bollinger and Duffie, 1988). Let $G_{sub}(s)$ be the system stabilized by PD-controller, and $G_{ff}(s)$ be the feedforward controller. Then the transfer function between the reference input, $V_r(s)$, and the system output, $V_q(s)$ is given as

$$\frac{V_q(s)}{V_r(s)}=\left(\frac{1+G_{ff}(s)}{G_I(s)}\right)\frac{G_I(s)G_{sub}(s)}{1+G_I(s)G_{sub}(s)} \tag{11}$$

Table 1 Identified parameters of the AMB-spindle system

Direction	Bias Current[A]		K_i	K_y
	I_{01}	I_{02}	[N/A]	[N/mm]
Y_1	2.16	1.52	187	356
Z_2	1.50	1.72	156	256
Y_2	2.25	1.70	193	378
Z_2	1.65	1.64	169	275

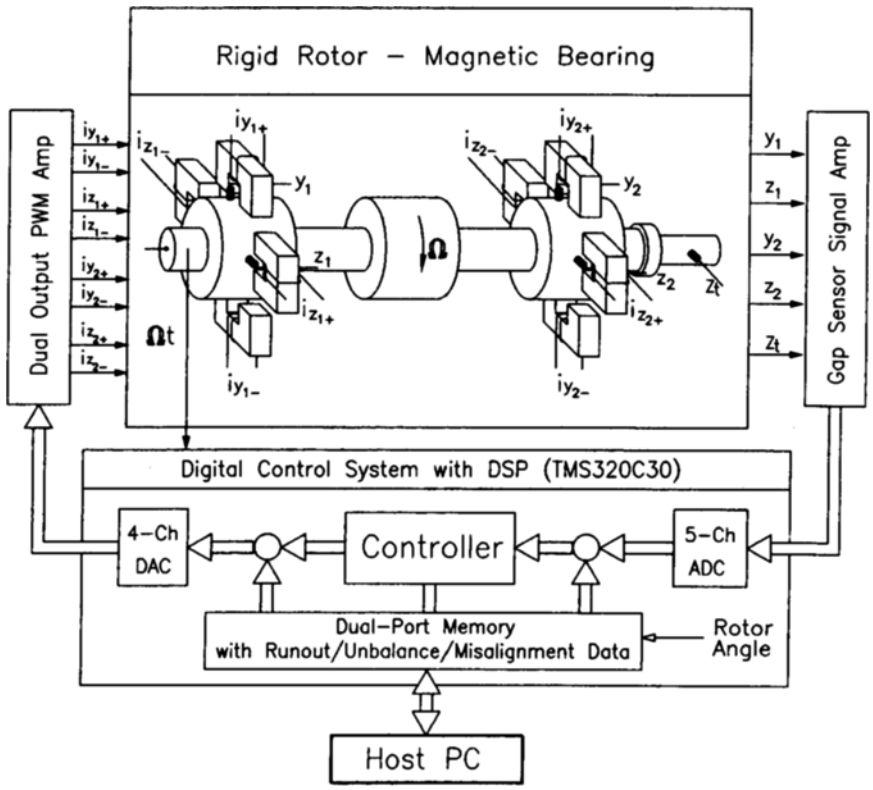

Fig. 4 Schematics of AMB-spindle system with digital controller

Table 2 Specifications of the designed AMB-spindle and digital control system

Electro-Magnet and Rotor	
Pole face area	A_p=450mm²(30×15)
Radial air gap/Rotor diameter	g_0=0.88mm/ϕ89mm
Magnetic coils	N=300turns, R=2Ω, L_0=56mH
Core lamination	0.35mm thick, 3% Si-steel
Geometric factor	$c=\alpha$=0.92
Rotor mass	m=8.34kg
Polar mass moment of inertia	J_P=0.0914kg · m²
Diametrical moment of inertia	J_d=0.00788kg · m²
Bearing span	b_1=139, b_2=138, b_t=277[mm]
Peripheral Electronic Devices	
Sensor & Amp.	Eddy current type, Resolution:0.5μm Gain K_s=5V/mm, Bandwidth=20kHz
PWM Power Amp.	Gain: K_c=0.42 A/V at 60Hz Bandwidth: 0~400Hz Output: 150V 10A, S/W Freq.: 18.5kHz
Motor/Drive	Output: 3ϕ 220V 16A Freq.: 3333Hz max (200,000rpm) Motor: 1.5kW 3ϕ Induction Motor
Encoder	360 pulses/rev. A&Z pulses used Input using DSP serial port
Degital Controller	
DSP	Floating point DSP: TMS320C30 Max. Perormance: 33MFLOPS 16.7MIPS
A/D converter	12bits 4ch. simultaneous sampling Input range: ±2.5V
D/A converter	12bits 16channel, synchronous update Output range: ±8.192V

where $G_I(s)=K_I/s$. Note that, if $G_{ff}(s)=1/G_{sub}(s)$, then $V_r(s)=V_q(s)$ in Eq. (11), leading to an ideal tracking performance. Because a feedforward control is essentially an open-loop control, the control performance depends on the accuracy of knowledge of the process transfer function. Figure 3 compares the FRFs of the PDF controlled system without and with feedforward controller. Although a perfect tracking, at least in theory, can be accomplished, tracking error is generated in practice because we don't exactly know the inverse dynamics of the system. In this work, the inverse dynamics is constructed by using the system parameters, which were previously identified experimentally (Kim, 1995; Kim and Lee, 1996a). The identified parameters are given in Table 1. When the identified parameters have uncertainties, an adaptation algorithm is required to compensate the error induced by the identification.

4. Experiment and Discussion

4.1 Experimental setup

Figure 4 shows the schematic of the rigid-AMB system with digital controller. Table 2 gives the specification of the tested AMB system. Figure 5(a) is a perspective view of the tested AMB-spindle system. A 50mm long tool bar is joined at the end of the spindle shaft, as shown in Fig. 5(b), to simulate a misaligned tool. The displacement signal measured at the tool tip and the rotational angle are fed to the digital signal processor (DSP,

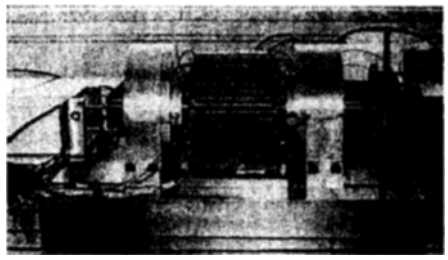

Fig. 5 (a) Perspective view of the experimental setup

Fig. 5 (b) The long tool bar and a gap sensor to simulate the tool misalignment

TS320C30) board via an analog to digital converter (ADC) and a counter, respectively. The DSP performs the 4-input/4-output PID-control action and simultaneously compensates for the tool axis misalignment and open loop rounout/unbalance (Kim and Lee, 1996b) by using the rotation synchronous encoder signal. The unbalance of shaft and the runout of sensor target using the open loop control was initially compensated. As the results, the system is operated within the $\pm 1 \mu m$ of shaft vibration and the residual vibration is only induced by the tool axis misalignment. The host PC downloads the instruction codes, the control gains, and the runout, unbalance and misalignment data, and monitors the operating condition of the AMB system, which is linked to the DSP via its dual-port memory for multi-tasking operation. The overall control period (frequency) is 50μsec (20kHz).

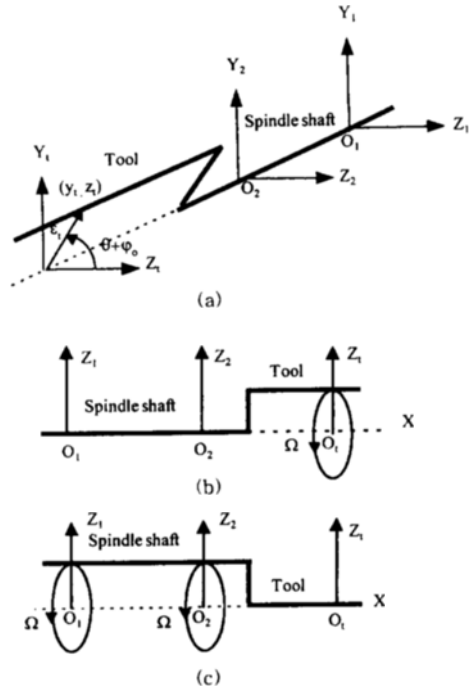

Fig. 6 Misalignment: (a) coordinate; (b) parallel misalignment; (c) compensation

4.2 Measurement and compensation scheme for misalignment

Figure 6(a) shows the coordinate system of the spindle shaft and the tool: $O_1Y_1Z_1$, $O_2Y_2Z_2$ and $O_tY_tZ_t$ are the coordinate systems for bearing #1, bearing #2 and the misaligned tool, respectively. The tool axis misalignment, in general, is the combination of parallel and angular misalignments. However, when the tool is in a point contact with work-piece during machining process, the tool axis parallel misalignment, which is shown in Fig. 6(b), will play a major role in machining inaccuracy. The compensation of the tested AMB system is limited by the air gap of 300 μm, between the emergency bearing and the spindle. To compensate for the parallel misalignment, the translational offset motion of the spindle shaft is used, as shown is Fig. 6(c). The tool axis misalignment can then be simplified as,

$$y_t(t) = \varepsilon_t sin(\theta + \varphi_o + \pi/2)$$
$$z_t(t) = \varepsilon_t sin(\theta + \varphi_o) \quad (12)$$

where $\theta = \Omega t$; φ_o is the initial angle of the tool

axis; Ω is the rotational speed; ε_t is the radius of parallel misalignment. In this work, the tool misalignment is measured near its tool tip, as shown in Fig. 5(b). The feedforward control input is added by using the inverse dynamics of the stabilized AMB-spindle system and the measured parallel misalignment signal.

4.3 Experimental results

Figure 7 shows the tracking performance at bearings #1 and #2 when the rotational speed is 2000rpm and the misaligned signal is given as the reference signal. As shown in Fig. 7(a), the ouput-to-input magnitude ratio is about 0.5, and the phase lag is about 100°, when the PDF-controller is used. Figure 7(b) shows the tracking performance when the feedforward controller is added to the existing PDF-controller. The phase lag, caused by the integral control action of PDF-controller, is drastically reduced by addition of the feedforward controller, and tracking performance is significantly improved through the full range of rotor angle.

Figure 8 shows the tool displacements when the

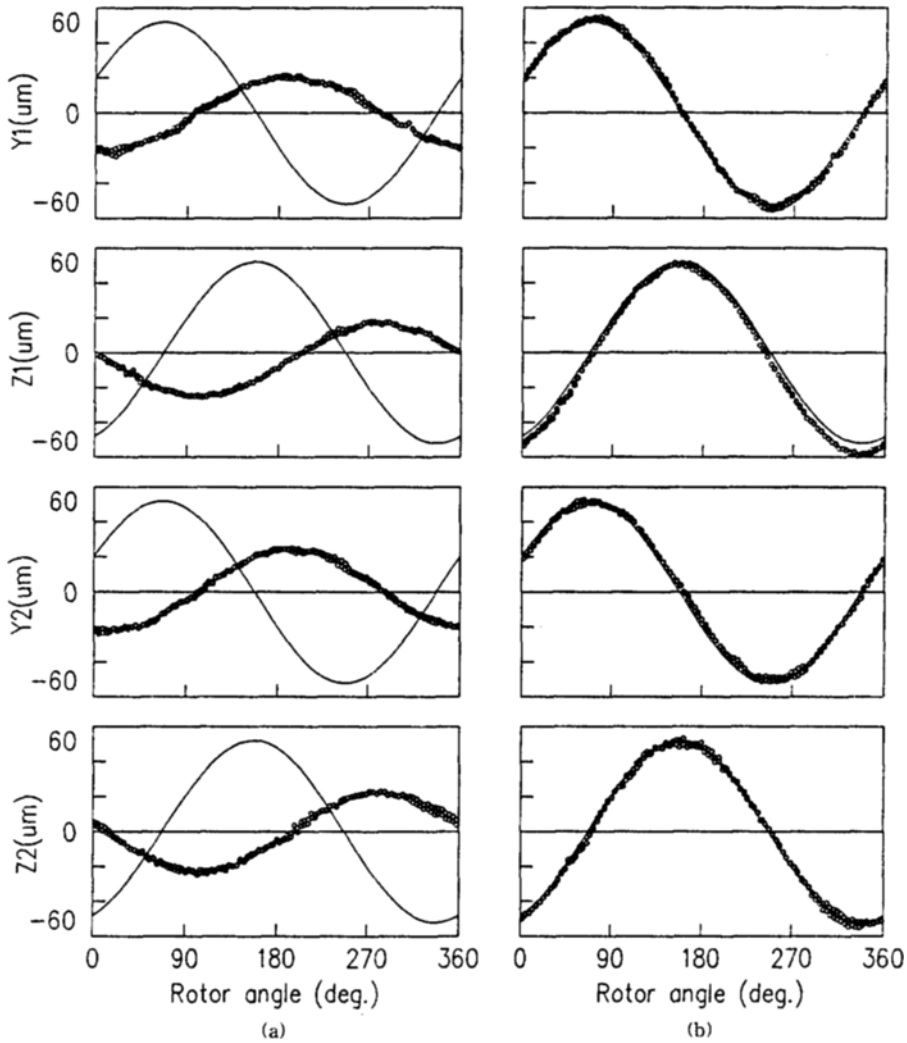

Fig. 7 Bearing responses at 2000rpm (a) without feedforward; (b) with feedforward ——— com mand, ∞∞∞∞ output response

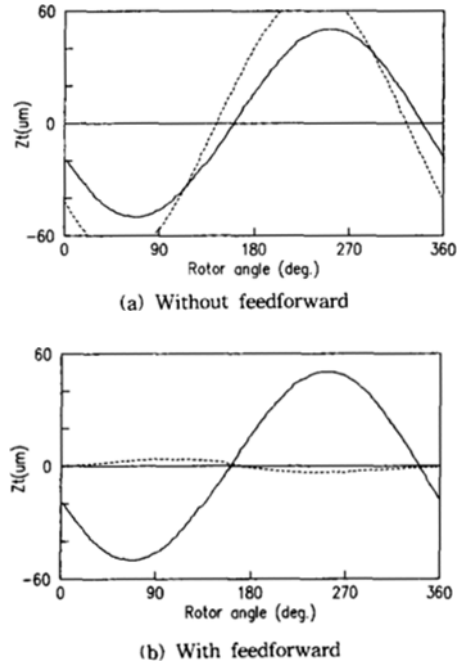

Fig. 8 Tool displacement at 2000rpm ; —— initial, ····· compensated

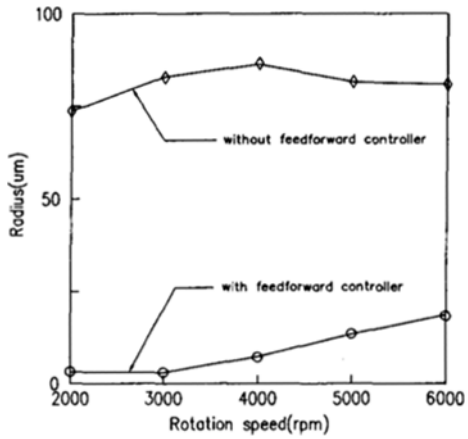

Fig. 9 Compensated tool displacement as the rotational speed is varied

AMBs track the reference input, where the solid and broken lines indicate the initial and compensated tool displacements, respectively. As shown in Fig. 8(a), the tool misalignment undesirably increases up to $\pm 73\mu m$ due to the large phase lag of the PDF controller. On the other hand, by adding the feedforward controller to the existing PDF controller, the initial tool displacement reduces to $\pm 3.3\mu m$, as shown in Fig 8(b).

Figure 9 shows the results of the compensation with/without the feedforward controller as the rotational speed is varied. Note that the misalignment can be reduced to less than $\pm 10\mu m$, at 4000rpm. However, as the spindle speed is increased further, the tracking performance of AMB becomes poor due to the increased phase lag, wich is due to the imperfect mathematical model without the consideration of gyroscopic effect.

5. Conclusions

The in-situ compensation of tool axis misalignment in a machine tool spindle system supported by rolling element bearings is not possible. On the other hand, for an AMB-spindle system, the parallel misalignment can be effectively compensated by tracking control of the spindle shaft within the air gap between the emergency bearing and the spindle shaft.

A pseudo-derivative feedback controller with feedforward input is proposed to exactly compensate the tool axis misalignment of the AMB-spindle system. A feedforward controller is constructed by inverting the AMB-spindle system dynamics which was stabilized by a PD-controller only. Although a perfect tracking, at least in theory, can be accomplished, tracking error is generated in practice because we don't exactly know the inverse dynamics of the system. The experimental results show that the proposed control scheme effectively compensates for the tool axis misalignment compared with the conventional PDF control scheme.

References

Bollinger, J. G. and Duffie, N.A., 1998, *Computer Control of Machine and Process*, Addeson Wesley, pp. 142~149.

Delprete, C., Genta, G. and Carabelli, S., 1994, "Control Strategies for Decentralized Control of

Active Magnetic Bearings," *Proceedings of the 4th International Symposium on Magnetic Bearings*, Switzerland, pp. 29~34.

Kim, C. S., 1995, Dynamic analysis and Isotropic Optimal Control of Active Magnetic Bearing System, Ph.D Dissertation, Department of Mechanical Engineering, KAIST, Korea.

Kim, C. S. and Lee, C. W., 1996a, "Isotropic Optimal Control of Active Magnetic Bearing System," *ASME Journal of Dynamic System, Measurement and Control*, (to appear in Vol. 118, No. 4, December 1996).

Kim, C. S. and Lee, C. W., 1996b, "In-situ Runout Identification in Active Magnetic Bearing System by Extended Influence Coefficient Method," *IEEE/ASME Journal of Mechatronics* (revised).

Möller, B., 1990, "Using High-Speed Electrospindles with Active Magnetic Bearings for Boring of Noncircular Shapes," *Proceedings of the 2nd International Symposium on Magnetic Bearings*, Tokyo, pp. 189~196.

Ota, M., Ando, S. and Oshima, J.-I., 1990, "Monitoring and Actuating Function of the Internal Grinding Spindle with Magnetic Bearings," *Proceedings of the 2nd International Symposium on Magnetic Bearings*, Tokyo, pp. 205~210.

Siegwart, R., Lasonneur, R. and Traxler, A., 1990, "Design and Performance of a High Speed Milling Spindle in Digitally Controlled Active Magnetic Bearing," *Proceedings of the 2nd International Symposium on Magnetic Bearings*, Tokyo, pp. 197~204.

Takita, Y. and Seto, K., 1991, "Investigation of Magnetic Bearing using LQI Theory," *Asia-Pacific Vibration Conference*, Vol. 3, pp. 33~37.

TMS320C3X User's Guide, Texas Instruments, 1992.